Theoretical Analysis of Linear Two-Dimensional Single Component Reactive Liquid Chromatography Model

Ugochukwu David Uche[1], Adetunji Kolawole Ilori[2], Toritsesan Brenda Batubo[3]

[1]Mathematics Programme, National Mathematical Centre Abuja, Nigeria

[2]Department of Mathematics University of Abuja, Abuja, Nigeria

[3]Statistics Programme, National Mathematical Centre Abuja, Nigeria

[4]Department of Mathematics, University of Benin, Nigeria

DOI: https://doi.org/10.51584/IJRIAS.2024.910018

Received: 02 October 2024; Accepted: 17 September 2024; Published: 09 November 2024

ABSTRACT

Semi-analytical solutions for a linear two-dimensional reactive general rate model of liquid chromatography is presented in this work considering cylindrical geometry. The governing model equations comprises of a system of advection-diffusion-reaction partial differential equations together with an algebraic expression representing the isothermal relation. The solutions are obtained by the application of finite Hankel and Laplace transforms one after the other. Moments are numerically obtained and used to describe the shapes of the elution profiles. A high-resolution finite volume scheme is lastly applied to obtain approximatesolutions of the governing model equations in order to verify the accuracy of the semi-analytical solutions. Several test cases are carried out and both the semi-analytical and numerical results are shown to have good agreements.

Key words: Reactive liquid chromatography, general rate model, semi-analytical solutions, numerical solutions.

INTRODUCTION

Liquid chromatography is a powerful technique widely used in the chemical and pharmaceutical industries for the separation and characterization of various substances. It is a method that allows the separation of a sample into its individual components based on their interactions with the mobile and stationary phases. The most common type of liquid chromatography is liquid-solid column chromatography, where a liquid mobile phase passes through a solid stationary phase to separate different components. Reactive liquid chromatography is a specialized technique that combines the principles of liquid chromatography with chemical reactions [1]. In this method, a reactive species is added to the mobile phase, which reacts with the analyte molecules as they pass through the column. This reaction can lead to changes in the analyte's chemical properties, such as its charge or polarity, facilitating its separation from other components in the mixture.

Reactive liquid chromatography offers several advantages over traditional liquid chromatography methods. Firstly, it allows for selective and specific separation of analytes based on their reactivity. This is particularly useful when dealing with complex mixtures containing closely related compounds. By exploiting the differences in their reactivity, reactive liquid chromatography can achieve better resolution and separation efficiency [2, 3]. In this cur- rent work, we study the effects of the reaction coefficient on elution for a single component operating under an isothermal condition.

Mathematical modeling of reactive liquid chromatography plays a crucial role in under- standing and optimizing separation processes in the various industries where the techniques are applicable. This powerful analytical technique uses chemical reactions to enhance the separation of compounds, making it a valuable tool in pharmaceutical, environmental, and food analysis. By developing mathematical models, deeper

ISSN No. 2454-6194 | DOI: 10.51584/IJRIAS |Volume IX Issue X October 2024

insights into the complex interactions occurring between the solutes, solvents, and stationary phase in reactive liquidchromatography columns can be gained [4–6]. Various models which are characterized by their level of complexities and used to describe the reactive liquid chromatography processcan be found in the literature [7–16]

This work extends the work recently done on one-dimensional reactive single component model by [17] to the two-dimensional model which considers both axial and radial concentration gradients. Analytical solutions of the governing model equations are derived by applying the Hankel and Laplace transformations successively together with the conventional solution technique for ODEs [18, 19]. These solutions are obtained for two kinds of boundary conditions namely Dirichlet and Danckwerts. It is not feasible to perform analytical inversions of the derived solutions because they contain complex functions. As a result, numerical Hankel and Laplace inversions are employed to convert the solutions backto their initial radial and time coordinates [20, 21]. In order to confirm the accuracy of the obtained solutions, numerical solutions are also acquired using a semi-discrete finite volume scheme (FVS) with high resolution, applied to the model governing equations [22, 23]. Test cases are carried out considering some kinetic parameters that influence the separation of solute in the column. The behavior of the chromatographic reactor is analyzed further by numerically calculating the moments of the concentration profile [24, 25].

The usefulness of the current two-dimensional model can be identified when at the time of solute injection at the column inlet, radial profile is introduced due to inexact injection, a non-homogeneously packed column and a larger column radius. These situations may occur in real life operations but are mostly neglected and thus, the application of a one- dimensional model. However, the current two-dimensional model can be a very reliable quantitative tool for more accurate predictions in liquid chromatography.

The article is further arranged in the following manner. In Section 2, a linear two- dimensional reactive general rate model of liquid chromatography is formulated and closed with the required initial and suggested boundary conditions. In Section 3, the analytical solutions for the two boundary conditions are obtained. Section 4 provides the test cases carried out and lastly in Section 5, the conclusion of the findings are given.

Linear two-dimensional reactive general rate model

An isothermal adsorption column filled with spherical particles of radius R_p is considered. Here, let t, z and r represent the time coordinate, axial coordinate along the column length and the radial coordinate along the column radius respectively.

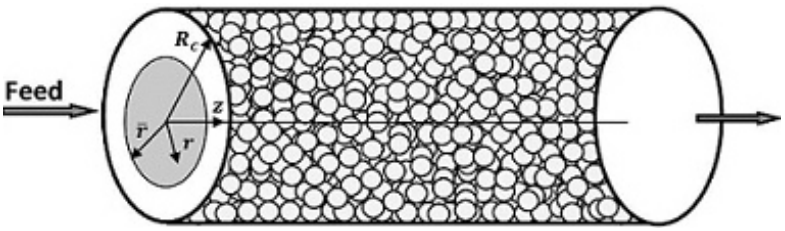

Figure 1: Schematic representation of a chromatographic column of cylindrical geometry packed with uniform sized particles

The solute is taken to travelin the z-direction (see Figure 1) by means of advection and axial dispersion, while being dispersed along the radius of the column. The following injection types are also assumed in order to project the radial mass transfer effects by dividing the inlet cross section of the column into an inner cylindrical core and an outer annular ring with the introduction of a new parameter r̃. This then leads to the possibility of injecting the solute through the inner core, the outer ring or through the whole cross-section. If r̃ is set equal to the radius of the column R_c, then we have the case where the injection of solute is carried out through the whole cross-section and this represents the scenario where there are no radial gradients introduced into the column, and thus can be represented by a simpler one-dimensional model, see [17]. The mass balance equations for the mobile phase of adsorption are given as

ISSN No. 2454-6194 | DOI: 10.51584/IJRIAS |Volume IX Issue X October 2024

$$\frac{\partial c}{\partial t} + u\frac{\partial c}{\partial z} = D_z\frac{\partial^2 c}{\partial z^2} + D_r\left(\frac{\partial^2 c}{\partial r^2} + \frac{1}{r}\frac{\partial c}{\partial r}\right) - \frac{3}{R_p}Fk_e(c - c_p|_{r_p=R_p}), \quad (1)$$

where c is the concentration in the bulk of fluid, c_p is the concentration in the particle pores, u is the interstitial velocity, D_z is the axial dispersion coefficient and $F = (1-\epsilon)/\epsilon$ is the phase ratio with ϵ as the external porosity. Moreover, D_r represents the radial dispersion coefficient and k_e is the external mass transfer coefficient. Lastly, r_p denotes the radial coordinate of spherical particles of radius R_p.

The corresponding mass balance equation inside the pores of the particles is given as

$$\epsilon_p\frac{\partial c_p}{\partial t} + (1-\epsilon_p)\frac{\partial q_p}{\partial t} = \frac{\epsilon_p D_p}{r_p^2}\frac{\partial}{\partial r_p}\left(r_p^2\frac{\partial c_p}{\partial r_p}\right) - (1-\epsilon_p)vq_p, \quad (2)$$

where D_p is the pore diffusivity, ϵ_p is the internal porosity and v is the reaction rateconstant of the solid phase. The equilibrium linear adsorption isotherm used in this study is the Langmuir isotherm expressed as

$$q_p = ac_p \quad (3)$$

where a denotes the linear adsorption or Henry's constant. The following dimensionless variables are introduced:

$$x = \frac{z}{L},\ \tau = \frac{ut}{L},\ \rho = \frac{r}{R_c},\ \rho_p = \frac{r_p}{R_p},\ Pe_z = \frac{Lu}{D_z},\ Pe_\rho = \frac{R_c^2 u}{D_{rL}},$$

$$\zeta = \frac{k_e R_p}{D_p},\ \eta = \frac{\epsilon_p D_p L}{R_p^2 u},\ \xi = 3\zeta\eta F,\ \omega = \frac{L}{u}v. \quad (4)$$

L is the characteristic column length, Pe_z and Pe_ρ denote the axial and radial Peclet numbers respectively, η and ξ, are the dimensionless constants, ζ denotes the coefficient of mass transfer and ω represents the dimensionless reaction rate constant. After applying the above dimensionless variables in Eqs. (1) and (2), the following system

of equations is obtained

$$\frac{\partial c}{\partial \tau} + \frac{\partial c}{\partial x} = \frac{1}{Pe_z}\frac{\partial^2 c}{\partial x^2} + \frac{1}{Pe_\rho}\left(\frac{\partial^2 c}{\partial \rho^2} + \frac{1}{\rho}\frac{\partial c}{\partial \rho}\right) - \xi(c - c_p|_{\rho_p=1}), \quad (5)$$

$$a^*\frac{\partial c_p}{\partial \tau} = \frac{\eta}{\rho_p^2}\frac{\partial}{\partial \rho_p}\left(\rho_p^2\frac{\partial c_p}{\partial \rho_p}\right) - a(1-\epsilon_p)\omega c_p, \quad (6)$$

where $a^* = \epsilon_p + a(1-\epsilon_p)$.

To close the system, the following initial conditions are defined for the system of equations:

$$c(\rho, x, \tau = 0) = 0, \qquad 0 \le x \le 1, \quad 0 \le \rho \le 1, \quad (7)$$

$$c_p(\rho_p, \rho, x, \tau = 0) = 0, \qquad 0 \le x \le 1, \quad 0 \le \rho \le 1, \quad 0 \le \rho_p \le 1. \quad (8)$$

The following boundary conditions for Eq. (5), which correspond to the symmetry of radialprofile and the impermeability of the column wall, are used along the radial coordinate ofthe column at $\rho = 0$ and $\rho = 1$:

$$\frac{\partial c(\rho=0,x,\tau)}{\partial \rho} = 0, \qquad \frac{\partial c(\rho=1,x,\tau)}{\partial \rho} = 0. \quad (9)$$

Also, for Eq. (5), the following two types of boundary conditions are considered.

ISSN No. 2454-6194 | DOI: 10.51584/IJRIAS |Volume IX Issue X October 2024

Danckwerts inlet boundary conditions:

For rectangular pulse injection through the inner cylindrical core, the boundary conditions are expressed as:

$$-\frac{1}{Pe_z}\frac{\partial c}{\partial x}+c|_{x=0}=\begin{cases}c^{inj}, & 0\le\rho\le\tilde{\rho} \quad and \quad 0\le\tau\le\tau_{inj},\\ 0, & \tilde{\rho}\le\rho\le 1 \quad or \quad \tau>\tau_{inj.}\end{cases} \tag{10}$$

And injecting the solute through the outer core, the boundary conditions are:

$$-\frac{1}{Pe_z}\frac{\partial c}{\partial x}+c|_{x=0}=\begin{cases}c^{inj}, & \tilde{\rho}\le\rho\le 1 \quad and \quad 0\le\tau\le\tau_{inj},\\ 0, & 0\le\rho\le\tilde{\rho} \quad or \quad \tau>\tau_{inj.}\end{cases} \tag{11}$$

$\tilde{\rho}=1$ in Eq. (10) or $\tilde{\rho}=0$ in Eq. (11) leads to inlet injection through the whole cross-section. c^{inj} is the injected concentration.

The above boundary conditions are coupled with the following Neumann conditions at the outlet of a finite length column

$$\frac{\partial c(\rho,x=1,\tau)}{\partial x}=0. \tag{12}$$

Dirichlet inlet boundary conditions:

When the dispersion coefficient D_z is small (i.e. for large values of the axial Peclet number Pe_z), the boundary conditions expressed in Eqs. (10) to (12) reduces to the Dirichlet boundary conditions as the quantity $-\frac{1}{Pe_z}\frac{\partial c}{\partial x}$ in the Danckwerts boundary conditions tend to zero. For large axial dispersion, the Danckwerts boundary conditions are more reliable to account for back flow near the left boundary.

Lastly, to take care of Eq. (6), the following boundary conditions at the end of the radial coordinates of the particles $\rho_p = 0$ and $\rho_p = 1$ are expressed as

$$\frac{\partial c_p}{\partial \rho_p}|_{\rho_p=0}=0, \qquad \frac{\partial c_p}{\partial \rho_p}|_{\rho_p=1}=\zeta\left(c-c_p|_{\rho_p=1}\right). \tag{13}$$

Semi-analytical solutions

To obtain the solutions of the above chromatographic model together with the described initial and boundary conditions, the finite Hankel and Laplace transforms are applied one after the other. The zeroth-order finite Hankel transform of $c(\rho, x, \tau)$ is defined as [18, 19]

$$c_H(\lambda_n,x,\tau)=H[c(\rho,x,\tau)]=\int_0^1 c(\rho,x,\tau)J_0(\lambda_n\rho)\rho d\rho. \tag{14}$$

The inverse Hankel transform is given as

$$c(\rho,x,\tau)=2c_H(\lambda_n=0,x,\tau)+\frac{2\sum_{n=1}^{\infty}c_H(\lambda_n,x,\tau)J_{0(\lambda_n\rho)}}{|J_{0(\lambda_n)}|^2}. \tag{15}$$

Applying the above Hankel transformation on Eq. (5) with respect to the coordinate ρ gives

$$\frac{\partial c_H}{\partial \tau}+\frac{\partial c_H}{\partial x}=\frac{1}{Pe_z}\frac{\partial^2 c_H}{\partial x^2}-\frac{\lambda_n^2}{Pe_\rho}c_H-\xi\left(c_H-c_{p,H}|_{\rho_p=1}\right). \tag{16}$$

Where $c_H(\lambda_n, x, \tau)$ and $c_{p,H}(\lambda_n, x, \tau)$ are the zeroth-order finite Hankel transforms of $c(\rho, x, \tau)$and $c_p(\rho_p, \rho, x, \tau)$, respectively. Next, the Laplace transformation of Hankel transformed function c_H is defined as [19]

ISSN No. 2454-6194 | DOI: 10.51584/IJRIAS |Volume IX Issue X October 2024

$$\bar{c}_H(\lambda_n, x, s) = \int_0^{\infty} e^{-\square\square} \square_{\square}(\square_{\square}, \square, \square)\square\square, \qquad \square \geq 0. \tag{17}$$

Applying the Laplace transformation on Eq. (16) with respect to τ while considering the initial concentration as zero to obtain

$$\square\square_{\square} \frac{\square\bar{\square}_{\square}}{\square\square} = \frac{\square^2\bar{\square}_{\square}}{\square\square^2} - \square\square_{\square}(\square + \frac{\square_{\square}^2}{\square\square_{\square}})\bar{\square}_{\square} - \square\square_{\square}\square\left(\bar{\square}_{\square} - \bar{\square}_{\square,\square}|_{\square_{\square}=1}\right). \tag{18}$$

Here, $\bar{c}_H$ is the Hankel and Laplace transformed concentration.

Applying the Laplace transform on Eq. (6) and rearranging the equation gives

$$\frac{\square^2}{\square\square_{\square}^2}(\square_{\square}\bar{\square}_{\square}) - \frac{\square^*\square}{\square}(\square_{\square}\bar{\square}_{\square}) + \frac{\square(1-\square_{\square})\square}{\square}(\square_{\square}\bar{\square}_{\square}) = 0. \tag{19}$$

The general solution of Eq. (19) is obtained as:

$$\bar{\square}_{\square}(\square_{\square}, \square, \square, \square) = \frac{1}{\square_{\square}}(\square_1\square^{\sqrt{\square(\square)}\square_{\square}} + \square_2\square^{-\sqrt{\square(\square)}\square_{\square}}). \tag{20}$$

where, $\square(\square) = \frac{\square^*\square + \square(1-\square_{\square})\square}{\square}$.

The constants A_1 and A_2 are determined by applying the boundary conditions stated in Eq. (13) and are given as:

$$\square_{1,2} = \pm \frac{\frac{\square\bar{\square}}{2\square\square\square h\left(\sqrt{\square(\square)}\right)}}{\left[(\square-1)+\sqrt{\square(\square)}\,\square\square\square h\left(\sqrt{\square(\square)}\right)\right]}. \tag{21}$$

Thus, the solution in Eq. (17) at $\rho_p = 1$, becomes

$$\bar{\square}_{\square}|_{\square_{\square}=1} = \bar{\square}h(\square), \tag{22}$$

where

$$h(\square) = \frac{\square}{\left[(\square-1)+\sqrt{\square(\square)}\,\square\square\square h\left(\sqrt{\square(\square)}\right)\right]}. \tag{23}$$

The Hankel transform of Eq. (22) with respect to ρ, gives

$$\bar{\square}_{\square,\square}|_{\square_{\square}=1} = \bar{\square}_{\square}h(\square), \tag{24}$$

Putting Eq. (24) in Eq. (18), the following is obtained

$$\frac{\square^2\bar{\square}_{\square}}{\square\square^2} - \square\square_{\square}\frac{\square\bar{\square}_{\square}}{\square x} - \square\square_{\square}\square(\square, \square_{\square})\bar{\square}_{\square} = 0\,, \tag{25}$$

where

$$\square(\square, \square_{\square}) = \square + \frac{\square_{\square}^2}{\square\square_{\square}} + \square\big(1 - h(\square)\big). \tag{26}$$

The general solution of the above Eq. (22) is given below as

$$\bar{\square}_{\square}(\square_{\square}, \square, \square) = \square_1\square^{\square_1\square} + \square_2\square^{\square_2\square}, \tag{27}$$

where

ISSN No. 2454-6194 | DOI: 10.51584/IJRIAS |Volume IX Issue X October 2024

$$\square_{1,2} = \frac{\square\square_{\square}}{2}\left(1 \pm \sqrt{1 + \frac{4\square(\square,\square_{\square})}{\square\square_{\square}}}\right), \quad (28)$$

and $\square_1$ andD_2 are constant to be determined from the following Hankel and Laplace transformed boundary conditions. $\square_1$ is obtained with the plus sign on top while $\square_2$ results from the minus sign below.

Next is to obtain the Hankel and Laplace transformed Danckwerts boundary conditions by taking the Hankel transformation of Eqs. (10) and (12) which gives

$$-\frac{1}{\square\square_{\square}}\frac{\square\square}{\square\square} + \square_{\square}|_{\square=0} = \begin{cases} \square^{\square\square\square}\,\square(\square_{\square}), & 0 \le \square \le \square_{\square\square\square}, \\ 0, & \square > \square_{\square\square\square} \end{cases} \quad (29)$$

and

$$\frac{\square\square_{\square}(\square_{\square},\square=1,\square)}{\square\square} = 0. \quad (30)$$

Where

$$\square(\square_{\square}) = \begin{cases} \frac{\bar{\square}^2}{2}, & \square\square\ \ \square_{\square} = 0, \\ \frac{\bar{\square}}{\square_{\square}}\square_1(\square_{\square}\bar{\square}), & \square\square\ \ \square_{\square} \neq 0. \end{cases} \quad \text{and} \quad \square(\square_{\square}) = \begin{cases} (\frac{1}{2} - \frac{\bar{\square}^2}{2}), & \square\square\ \ \square_{\square} = 0, \\ -\frac{\bar{\square}}{\square_{\square}}\square_1(\square_{\square}\bar{\square}), & \square\square\ \ \square_{\square} \neq 0. \end{cases}$$

both represent inner and out core injections respectively.

Next, applying the Laplace transformation on the boundary conditions given in Eqs. (29) and (30), we obtain

$$-\frac{1}{\mathrm{Pe}_z}\frac{\partial c}{\partial x} + c_H|_{x=0} = \frac{c^{inj}Q(\lambda_n)}{s}(1 - e^{-s\tau_{inj}}) \quad (31)$$

and

$$\frac{\partial \bar{c}_H(\lambda_n,x=1,s)}{\partial x} = 0. \quad (32)$$

Now, plugging in the values from these boundary conditions obtained in Eqs. (31) and (32) into Eq. (27), we obtain the solution as

$$\bar{c}_H(\lambda_n, x, s) = \frac{(b_1 - b_2)e^{b_1 + b_2 x}\left[\frac{Q(\lambda_n)c^{inj}}{s}\left(1 - e^{-s\tau_{inj}}\right)\right]}{b_2 e^{b_2}\left(1 - \frac{b_1}{\mathrm{Pe}_z}\right) - b_1 e^{b_1}\left(1 - \frac{b_2}{\mathrm{Pe}_z}\right)}. \quad (33)$$

Following a similar procedure, the solution obtained by considering the Dirichlet boundary condition is given as

$$\bar{c}_H(\lambda_n, x, s) = \frac{Q(\lambda_n)c^{inj}e^{b_2 x}}{s}(1 - e^{-s\tau_{inj}}). \quad (34)$$

Numerical inversion approach is used to convert the above two solutions back into the original coordinates [20,21].

Numerical case studies

In this section, several test cases are studied to verify the accuracy of the semi-analytical solutions and to study the effects of some parameters on the concentration profile. To obtain approximate solutions for the

ISSN No. 2454-6194 | DOI: 10.51584/IJRIAS |Volume IX Issue X October 2024

governing model equations, the semi discrete high resolution finite volume scheme (HR-FVS) of Koren is implemented [22, 23, 25]. Parameters used for the test cases are taken from the ranges frequently used in liquid chromatography applications and are given in Table 1.

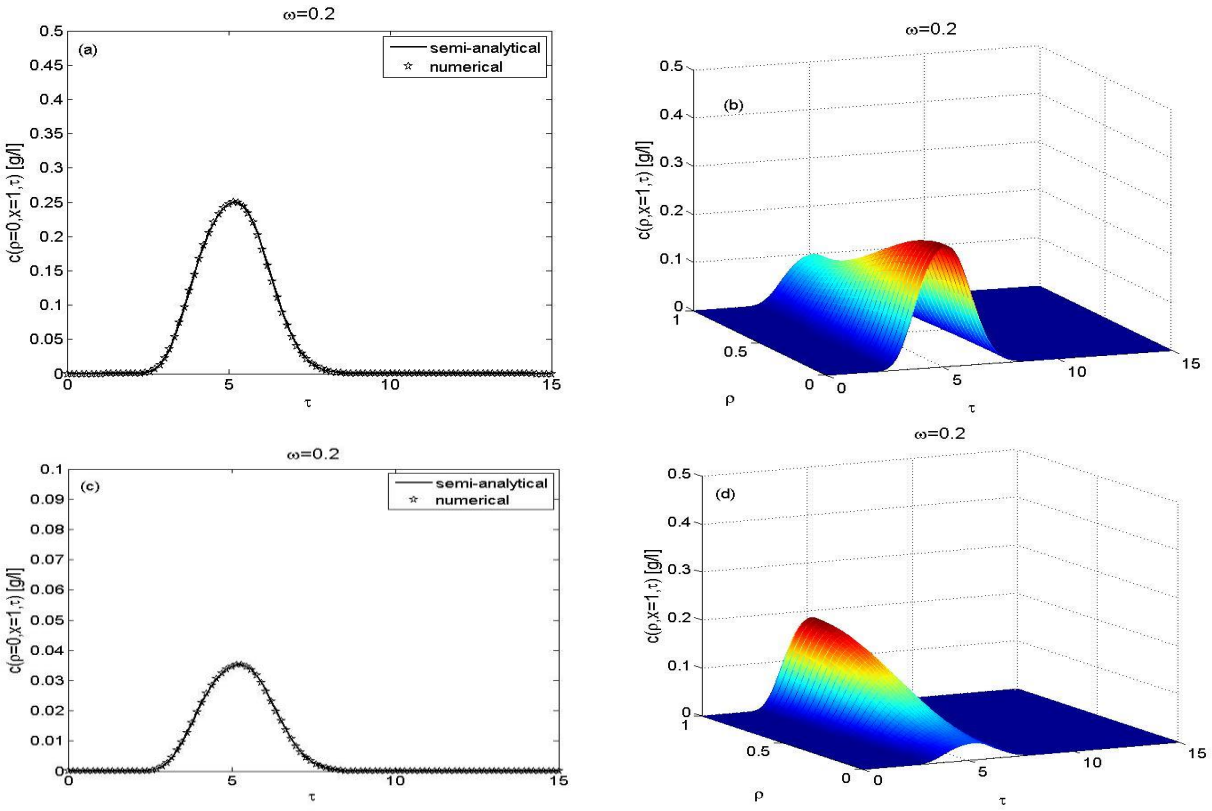

Figure 2: Effects of injection on the concentration profiles for 1d and 3d plots, through the inner core and outer ring for Dancwerts boundary condition

Figure 2 show one-dimensional (1d) and three-dimensional (3d) plots for the solutions resulting from injecting through the inner cylindrical core (Figures 2(a) and (b)) and via the outer annular ring (Figures 2(c) and (d)). The results were obtained using the Danckwerts boundary condition. The 1d plots show a good agreement between semi-analytical and the numerical solutions. The 3d plots are used to demonstrate the evolution of radial concentration profiles caused by slow radial dispersion. At the column outlet, due to slow radial dispersion (i.e. for $Pe_\rho = 15$), a higher concentration can be seen at the outer region as compared to the inner cylindrical region due to slow radial dispersion.

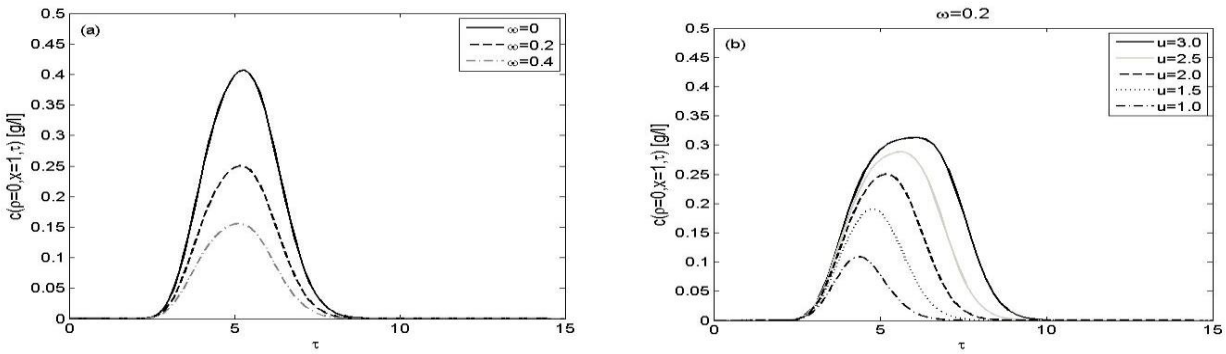

Figure 3: Effects of reaction rate constant ω and velocity u on the concentration profiles for inner core injection

Figure 3 display the effects of the reaction rate constant ω and velocity u on the concentration profiles for inner cylindrical core injection. The effect of ω as seen in Figure 3(a), shows that increasing the value of ω causes a reduced concentration profile. This shows that chemical reaction between sample

ISSN No. 2454-6194 | DOI: 10.51584/IJRIAS |Volume IX Issue X October 2024

components and the particle phase in the column increases. Hence the samples will be quickly converted to products as the reaction rate constant increases. Figure 3(b) gives the effects of increasing the velocity on the concentration profiles. It is evident that increasing the velocity leads to higher concentration profiles. This leads to faster elution and faster dispersion rates hence, causing less reaction due to less interaction time between the solute and the particle phase inside the column.

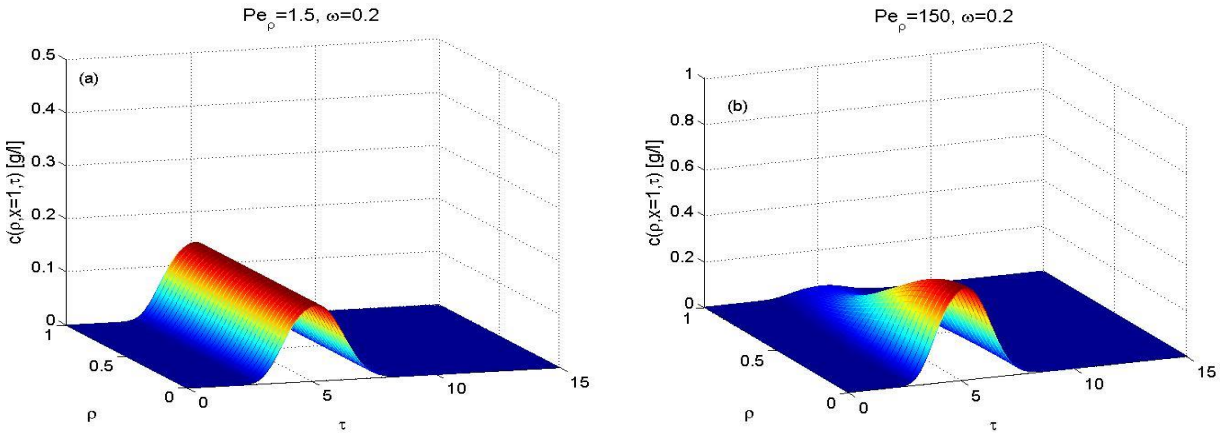

Figure 4: Effects of Peρ on the concentration profiles for injection through the inner core

In Figure 4, the radial dispersion coefficient Pe_ρ effect on the concentration profile is shown for inner cylindrical core injection. For small $Pe_\rho = 1.5$, which is the result shown in Figure 4(a), there is no visible effects on the concentration profile due to quicker radial dispersion. This case collapses the two-dimensional model to a one-dimensional model. On the other hand, the effects of slow radial dispersion (for $Pe_\rho = 150$) can be seen as the concentration profile reduces at the middle of the column in Figure 4(b).

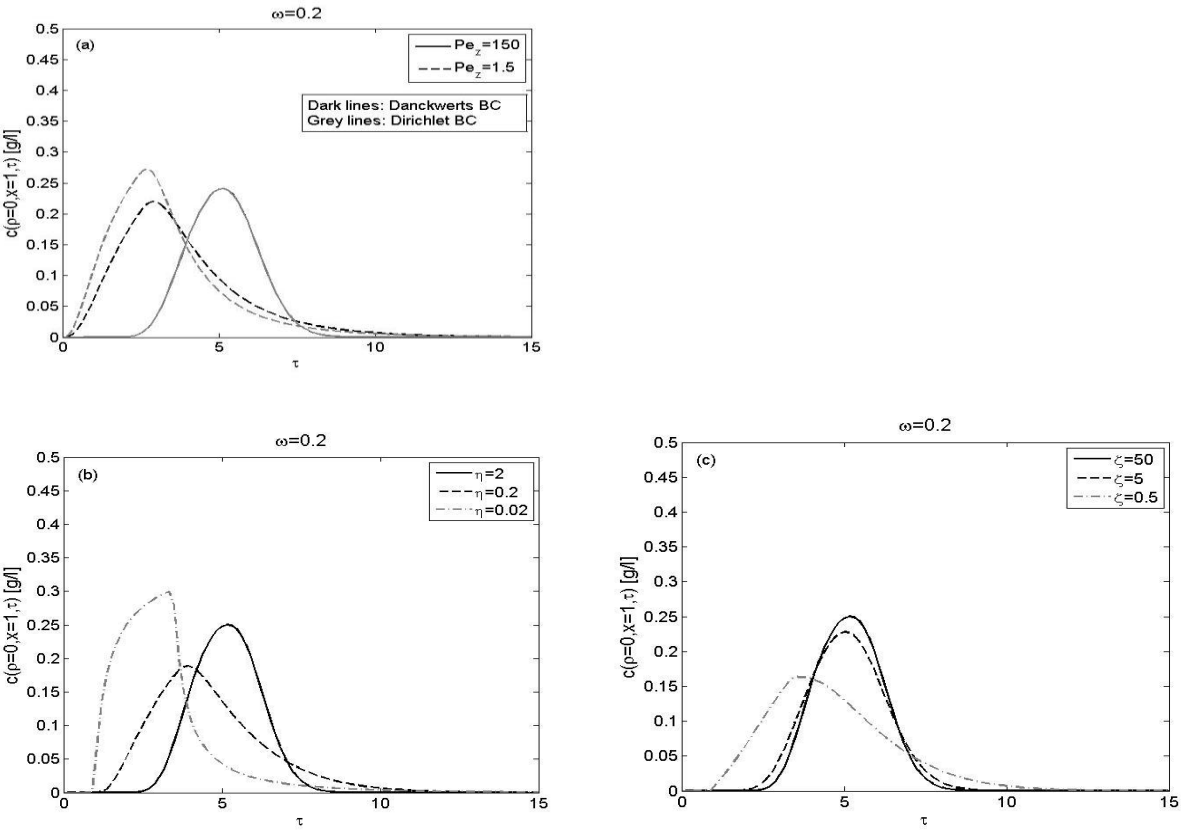

Figure 5: Effects of Pez coupled with the BCs, η and ζ on the concentration profiles for inner core injection

Figure 5 gives the effects of the axial dispersion coefficient Pe_z, intraparticle diffusion co- efficient η and mass transfer coefficient ζ on the concentration profiles plotted for inner cylindrical core injections. In Figure 5(a),

ISSN No. 2454-6194 | DOI: 10.51584/IJRIAS |Volume IX Issue X October 2024

Pe_z is altered to see the effects on the con- centration profiles for the solutions obtained from the two types of boundary conditions considered. It is seen that for small axial Peclet number $Pe_z = 1.5$, the solutions of both boundary conditions tend to differ and the retention times of the solutes increasesas broader profiles can be observed. The results in Figures 5(b) and 5(c) show similar behaviors in studying the effects of η and ζ respectively. It can be seen that reducing the values of each of η and ζ leads to broad tailed concentration profiles and hence leading to

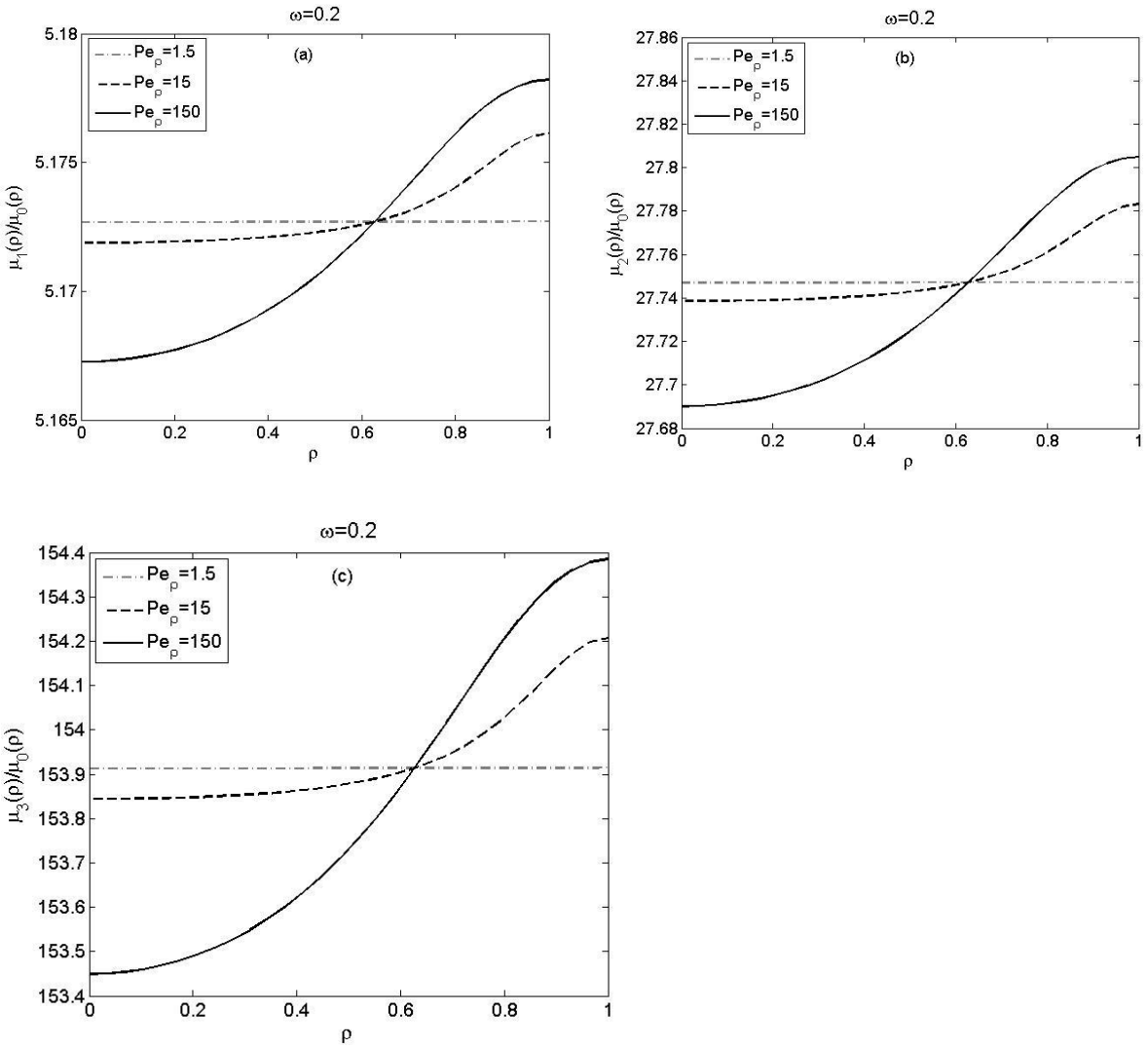

Figure 6: Effects of Peρ on the local moments for inner core injection

increased retention times inside the column.

Figures 6 and 7 show the results of the obtained numerical moments for inner cylindrical core injections. Moments analysis is very useful tool in describing the shapes of the concentration profiles. These moments were calculated numerically by using the following expressions [5]

$$\mu_{i,av} = \frac{\int_0^\infty c_{av}(x=1,\tau)\tau^i d\tau}{\mu_{0,av}}, \quad i = 2,3,4, \qquad (35)$$

where $\mu_{i,av}$ is given below for $i = 1$ as

$$\mu_{0,av} = \int_0^\infty c_{av}(x=1,\tau)d\tau \qquad (36)$$

and

ISSN No. 2454-6194 | DOI: 10.51584/IJRIAS |Volume IX Issue X October 2024

$$c_{av}(x,\tau) = 2\int_0^1 c(\rho, x=1, \tau)\rho d\rho. \qquad (37)$$

In Figure 6, the effect of the radial dispersion coefficient Pe_ρ on the local moments is shown. The results display that for the smallest value of Pe_ρ, the moments approach constant values along the radial coordinate. Due to the injection of the solute via the inner cylindrical core, there are no changes in the moments near the center of the column. The changes are however seen in the outer region of the column. An increase in Pe_ρ can be seen to cause larger changes in the higher moments. The results presented here are in good agreement with the results given in Figure 4.

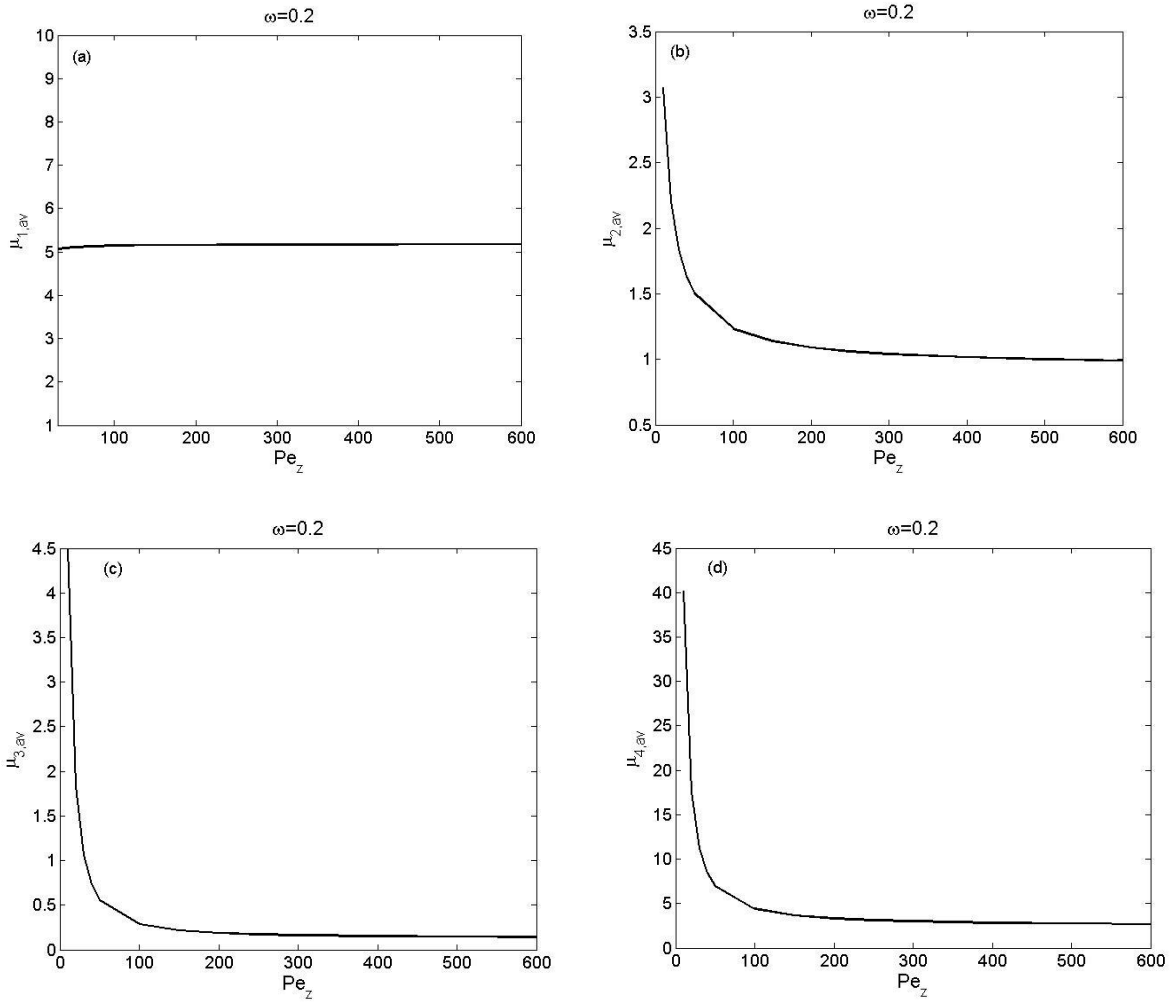

Figure 7: Effects of Pez on the averaged central moments for inner core injection

Figure 7 shows the axial dispersion coefficient Pe_z effects on the averaged moments. The results show that no visible effect can be observed on the first moment. On the otherhand, the effects can be seen on the other moments as the axial Peclet number is increased causing a reduction in the values of the moment. These results again are in good agreement with the results given in Figure 5(a).

Table 1: Standard parameters used in the test problems.

Parameter	Symbol	Value
Length of column	**L**	8.0 cm
External porosity	ϵ_b	0.4
Internal porosity	ϵ_p	0.333

ISSN No. 2454-6194 | DOI: 10.51584/IJRIAS |Volume IX Issue X October 2024

Interstitial velocity	u	2.0 cm/min
Axial dispersion coefficient	D_z, (Pe_z)	2.6667×10^{-2}cm^2/min, (600)
Radial dispersion coefficient	D_r, (Pe_ρ)	6.6667×10^{-4}cm^2/min, (15)
Henry's constant	a	2.5
Dimensionless constant	η	2
Dimensionless constant	ζ	50
Injected concentration	c^{inj}	0.5 [g/l]
Dimensionless time of injection	τ_{inj}	2.5

CONCLUSION

A linear two-dimensional reactive liquid chromatography model was solved analytically considering two types of boundary conditions. Semi-analytical solutions were obtained by the successive application of finite Hankel and Laplace transforms. The numerical inversions of Hankel and Laplace transforms were used to obtain the solutions in their true domains. A high resolution semi-discrete finite volume scheme was subsequently applied to obtain approximate solutions of the governing model equations in order to have confidence on the obtained semi-analytical solutions. Both the semi-analytical and the numerical solutions were seen to be in good agreement, this also validates the accuracy of numerical scheme used. The obtained two-dimensional model solutions was shown to capture the scenario where radial gradients are introduced during injection of solutes inside the chromatography columns and can play a significant role in further the developmentsof reactive chromatography processes.

REFERENCES

1. G. Agrawal, J. Oh, B. Sreedhar, S. Tie, M. E. Donaldson, T. C. Frank, A. K. Schultz, A. S. Bommarius & Y. Kawajiri, "Optimization of reactive simulated moving bed systems with modulation of feed concentration for production of glycol ether ester", Journal of Chromatography A 1360 (2014) 196-208.
2. S. Grüner & A. Kienle, "Equilibrium theory and nonlinear waves for reactive distillation columns and chromatographic reactors", Chemical Engineering Science 59 (2004)901-918.
3. T. Borren, J. Fricke & H. Schmidt-Traub, Integrated Reaction and Separation Operations, Springer, Berlin, Heidelberg 2006.
4. G. Guiochon, "Preparative liquid chromatography", Journal of Chromatography A 965 (2002) 129-161.
5. G. Guiochon, A. Felinger, D. G. Shirazi & A. M. Katti, Fundamentals of preparative and nonlinear chromatography, 2nd editon, ELsevier Academic Press, New York 2006.
6. J. C. Bellot & J. S. Condoretm, "Liquid Chromatography Modelling: A Review", Process Biochemistry 26 (1991) 363-376.
7. G. Carta, "Exact analytical solution of a mathematical model for chromatographic operations", Chemical Engineering Science 43 (1988) 2877-2883.
8. S. Qamar, S. Perveen, & A. Seidel-Morgenstern, "Numerical approximation of a two- dimensional nonlinear and nonequilibrium model of reactive chromatography", Indus- trial & Engineering Chemistry Research 55 (2016) 9003-9014.
9. S. Qamar, U. D. Uche, F. U. Khan & A. Seidel-Morgenstern, "Analysis of linear two-dimensional general rate model for chromatographic columns of cylindrical geometry", Journal of Chromatography A 1496 (2017) 92-104.

10. S. Qamar, S. Bibi, F. U. Khan, M. Shah, S. Javeed & A. Seidel-Morgenstern, "Irreversible and Reversible Reactions in a Liquid Chromatographic Column: Analytical Solutions and Moment Analysis", Industrial & Engineering Chemistry Research 53 (2014) 2461.
11. S. Bibi, S. Qamar & A. Seidel-Morgenstern, "Irreversible and reversible reactive chromatography: Analytical solutions and moment analysis for rectangular pulse injections", Journal of Chromatography A 1385 (2015) 49-62.
12. S. Parveen, S. Qamar & A. Seidel-Morgenstern, "Analysis of a two-Dimensional non- Equilibrium model of linear reactive Chromatography considering irreversible and reversible reactions", Industrial & Engineering Chemistry Research 55 (2016) 2471- 2482.
13. U. D. Uche, S. Qamar & A. Seidel-Morgenstern, "Numerical approximation of a nonisothermal two-dimensional general rate model of reactive liquid chromatography", International Journal of Chemical Kinetics 52 (2020) 134-155. https://doi.org/10.1002/kin.21337
14. A. G. Ahmad, N. F. Okechi, U. D. Uche & A. O. Salaudeen, "Numerical simulation of nonlinear and non-Isothermal liquid chromatography for studying thermal variations in columns packed with core-shell particles", Journal of Nigerian Society of Physical Sciences 5 (2023) 1350.
15. U. D. Uche, M. Uche, F. Okafor & K. Utalor, "Modeling and simulation of isothermal reactive liquid chromatography for two component elution effects of core-shell particles", International Journal of Mathematical Sciences and Optimization: Theory and Applications 8 (2022) 117.
16. U. D. Uche, M. Uche & F. Okafor, "Numerical solution of a two-dimensional model for non-isothermal chromatographic reactor packed with core-shell particles", Journal of the Nigerian Mathematical Society 3 (2021) 97.
17. K. A. M. Alharbi, S. Bashir, M. Ramzan, S. Kadry & S. M. Eldin, "Analysis of Liquid Chromatography Considering a Linear Single-Component Heterogeneous-Type Reactive General Rate Model", ACS Omega 8(37) (2023) 33280-33288.
18. H. S. Carslaw & J. C. Jaeger, Operational methods in applied mathematics, Oxford University Press, Oxford 1953.
19. I. H. Sneddon, The use of integral transforms, McGraw-Hill, New York 1972.
20. F. Durbin, "Numerical Inversion of Laplace Transforms: An efficient improvement to Dubner and Abate's Method", The Computer Journal 17 (1974) 371-376.
21. I. S. Chen, Y. -H. Liu, C. -P. Liang, C. -W. Liu & C. -W. Lin, "Exact analytical solutions for two-dimensional advection-dispersion equation in cylindrical coordinates subject to third-type inlet boundary conditions", Advances in Water Resources 34 (2011) 365-374.
22. B. Koren, "A robust upwind discretization method for advection, diffusion and source terms", in Numerical Methods for Advection-Diffusion Problems, Volume 45 of Notes on Numerical Fluid Mechanics, Vieweg Verlag, Braunschweig 1993, pp. 117-138.
23. S. Javeed, S. Qamar, A. Seidel-Morgenstern & G. Warnecke, "Efficient and accurate numerical simulation of nonlinear chromatographic processes", Journal of Computers & Chemical Engineering 35 (2011) 2294-2305.
24. S. Parveen, S. Qamar & A. Seidel-Morgenstern, "Two-dimensional non-equilibrium model of liquid chromatography: Analytical solutions and moment analysis", Chemical Engineering Science 122 (2015) 64-77.
25. U. D. Uche, S. Qamar & A. Seidel-Morgenstern, "Analytical and numerical solutions of two-dimensional general rate models for liquid chromatographic columns packed with core-shell particles", Chemical Engineering Research & Design 130 (2018) 295-320.